4

Semiannual Technical Report

Selected Energy Epitaxial Deposition and Low Energy Electron Microscopy of AlN, GaN and SiC Thin Films

Supported under Grant #N00014-95-1-0122
Office of the Chief of Naval Research
Report for the period 11/1/94–6/30/95

R. F. Davis, H. H. Lamb† and I. S. T. Tsong*,
E. Bauer*, R. B. Doak*, J. L. Edwards*, N. Freed*, S. Horch*,
C. Linsmeier*, M. Meloni*, K. E. Schmidt*, J. Sumakeris and V. Torres*
Materials Science and Engineering Department
†Chemical Engineering Department
*Arizona State University
North Carolina State University
Campus Box 7907
Raleigh, NC 27695-7907

June, 1995

REPORT DOCUMENTATION PAGE

Form Approved
OMB No. 0704-0188

1. AGENCY USE ONLY *(Leave blank)*	2. REPORT DATE	3. REPORT TYPE AND DATES COVERED
	June, 1995	Semiannual Technical 11/1/94–6/30/95

4. TITLE AND SUBTITLE
Selected Energy Epitaxial Deposition and Low Energy Electron Microscopy of AlN, GaN, and SiC Thin Films

5. FUNDING NUMBERS
1213801---01
312
N00179
N66020
4B855

6. AUTHOR(S)
R. F. Davis, H. H. Lamb and I. S. T. Tsong

7. PERFORMING ORGANIZATION NAME(S) AND ADDRESS(ES)
North Carolina State University
Hillsborough Street
Raleigh, NC 27695

8. PERFORMING ORGANIZATION REPORT NUMBER
N00014-95-1-0122

9. SPONSORING/MONITORING AGENCY NAMES(S) AND ADDRESS(ES)
Sponsoring: ONR, Code 312, 800 N. Quincy, Arlington, VA 22217-5660
Monitoring: Administrative Contracting Officer, Regional Office Atlanta
Regional Office Atlanta, 101 Marietta Tower, Suite 2805
101 Marietta Street
Atlanta, GA 30323-0008

10. SPONSORING/MONITORING AGENCY REPORT NUMBER

11. SUPPLEMENTARY NOTES

12a. DISTRIBUTION/AVAILABILITY STATEMENT
Approved for Public Release; Distribution Unlimited

12b. DISTRIBUTION CODE

13. ABSTRACT ***(Maximum 200 words)***

Investigations at North Carolina State University and Arizona State University concerned with the preparation of substrate surfaces, theoretical modeling of atom/surface collisions and subsequent growth mechanisms, design of new supersonic jet systems and ion beam technologies, and deposition of GaN films via supersonic processes have been conducted during this reporting period. Chemical etching and oxidation were examined in an unsuccessful attempt to remove scratches from the surfaces of 6H-SiC$(0001)_{si}$ and $(0001)_c$ substrates for use in growth of III-V nitride thin films. Quantum molecular dynamics of projectile molecules colliding with surfaces have been initiated to understand the processes ongoing when supersonic beams of atoms or molecules collide with a substrate surface. Growth processes at longer time scales are also being investigated using Monte Carlo simulation. The design of supersonic beam sources for use with LEEM characterization at ASU has been completed. The construction of a dual supersonic beam deposition system with an attached UHV analysis system is ongoing. A dual Colutron ion-beam system is also under construction for the deposition of SiC and GaN. Stoichiometric GaN films have been deposited on $Al_2O_3(0001)$, Si(001) and Si(111) substrates using an NH_3-seeded free He jet and an effusive triethylgallium (TEG) source. Very uniform films have been achieved at low temperatures.

14. SUBJECT TERMS
SiC, silicon carbide, chemical etching, oxidation, theoretical modeling, atom/surface collisions, Monte Carlo simulation, supersonic jet, supersonic beams, ion beams, low energy electron microscopy, LEEM, gallium nitride, GaN, aluminum nitride, AlN, ammonia, molecular beam epitaxy, MBE, MIS diodes, C-V measurements, dielectric constant

15. NUMBER OF PAGES
34

16. PRICE CODE

17. SECURITY CLASSIFICATION OF REPORT	18. SECURITY CLASSIFICATION OF THIS PAGE	19. SECURITY CLASSIFICATION OF ABSTRACT	20. LIMITATION OF ABSTRACT
UNCLAS	UNCLAS	UNCLAS	SAR

Table of Contents

I. Introduction

The realized and potential electronic applications of AlN, GaN and SiC are well known. Moreover, a continuous range of solid solutions and pseudomorphic heterostructures of controlled periodicities and tunable bandgaps from 2.3 eV (3C-SiC) to 6.3 eV (AlN) have been produced at North Carolina State University (NCSU) and elsewhere in the GaN-AlN and AlN-SiC systems. The wide bandgaps of these materials and their strong atomic bonding have allowed the fabrication of high-power, high-frequency and high-temperature devices. However, the high vapor pressures of N and Si in the nitrides and SiC, respectively, force the use of low deposition temperatures with resultant inefficient chemisorption and reduced surface diffusion rates. The use of these low temperatures also increases the probability of the uncontrolled introduction of impurities as well as point, line and planar defects which are likely to be electrically active. An effective method must be found to routinely produce intrinsic epitaxial films of AlN, GaN and SiC having low defect densities.

Recently, Ceyer [1, 2] has demonstrated that the barrier to dissociative chemisorption of a reactant upon collision with a surface can be overcome by the translational energy of the incident molecule. Ceyer's explanation for this process is based upon a potential energy diagram (Fig. 1) similar to that given by classical transition-state theory (or activated-complex theory) in chemical kinetics. The dotted and dashed lines in Fig. 1 show, respectively, the potential wells for molecular physisorption and dissociative chemisorption onto the surface. In general, there will be an energy barrier to overcome for the atoms of the physisorbed molecule to dissociate and chemically bond to the surface. Depending upon the equilibrium positions and well depths of the physisorbed and chemisorbed states, the energy of the transition state E^* can be less than zero or greater than zero. In the former case, the reaction proceeds spontaneously. In the latter case, the molecule will never proceed from the physisorbed state (the precursor state) to the chemisorbed state unless an additional source of energy can be drawn upon to surmount the barrier. This energy can only come from either (1) the thermal energy of the surface, (2) stored internal energy (rotational and vibrational) of the molecule, or (3) the incident translational kinetic energy of the molecule. Conversion of translational kinetic energy into the required potential energy is the most efficient of these processes. Moreover, by adjusting the kinetic energy, E_i, of the incoming molecule, it is possible to turn off the reaction ($E_i < E^*$), to tailor the reaction to just proceed ($E_i = E^*$), or to set the amount of excess energy to be released ($E_i > E^*$). The thrust of the present research is to employ these attributes of the beam translational energy to tune the reaction chemistry for wide bandgap semiconductor epitaxial growth.

The transition state, E^*, is essentially the activation energy for dissociation and chemisorption of the incident molecules. Its exact magnitude is unknown, but is most certainly

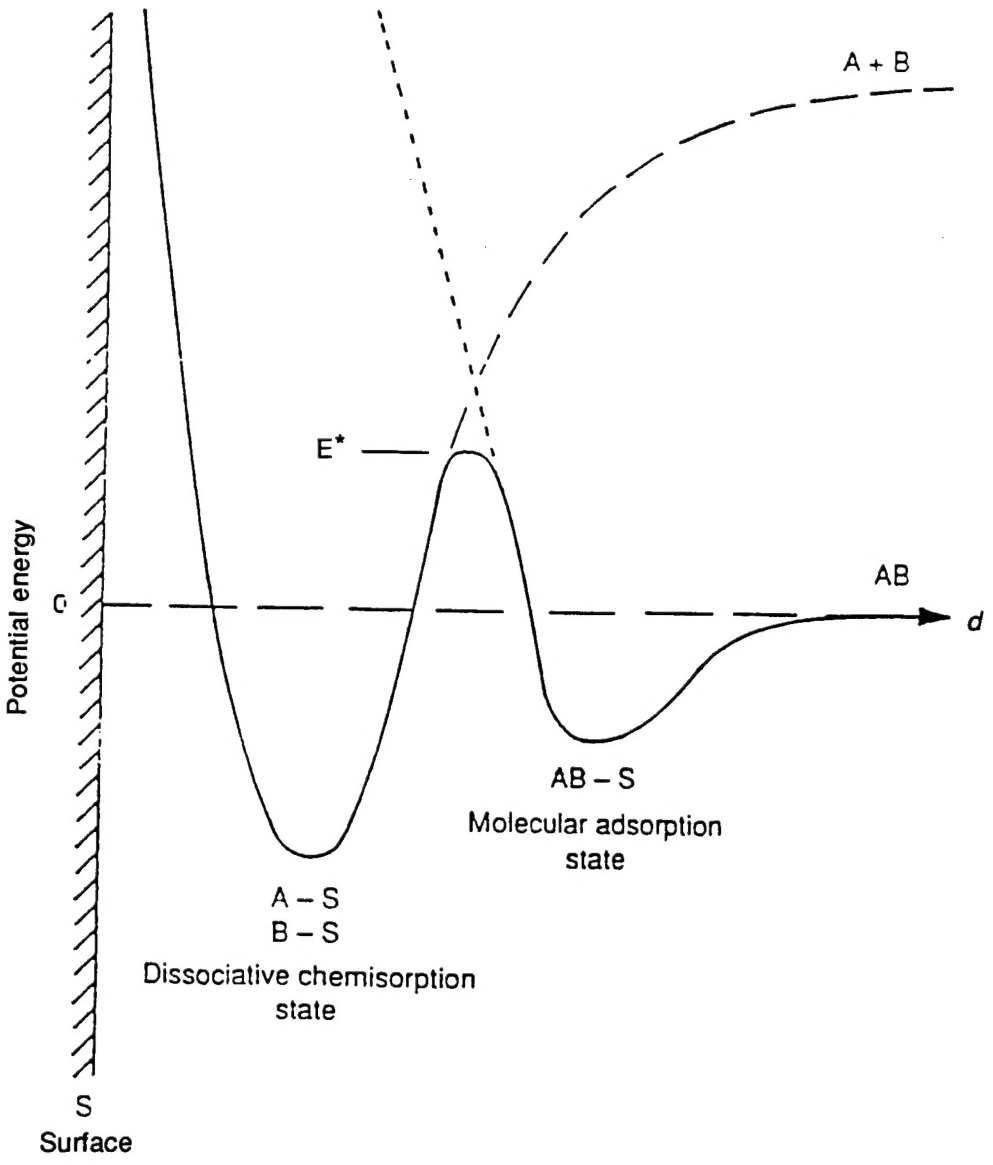

Figure 1. Schematic potential energy diagram of an activated surface reaction involving a molecularly physisorbed precursor state [from Ref. 1].

lower than the dissociation energy of the free molecule. It does not necessarily follow, however, that any kinetic energy above E^* will promote high-quality epitaxial growth of GaN. One must take into consideration another energy threshold, E_d, beyond which the kinetic energy of the incident flux will cause damage to the epitaxial film being synthesized. A typical E_d threshold value is approximately five times the bandgap of the crystal and in the case of GaN, $E_d \approx 18$ eV.

From the above consideration, it is clear that the key to high quality epitaxial growth is to be able to tune the energy of the incoming flux species over a range of energies defined by the window between E^* and E_d. Since the window is quite restrictive, i.e. 1-20 eV, it is essential

that the energy spread of the flux species must be small, i.e. the flux species should ideally be monoenergetic. To this end, we employ Selected Energy Epitaxial Deposition (SEED) systems for the growth of AlN, GaN and SiC wide bandgap semiconductors. The SEED systems are of two types: (1) a seeded-beam supersonic free-jet (SSJ) and (2) a dual ion-beam Colutron. Both these SEED systems have the desirable property of a narrow energy spread of ≤ 1 eV.

Epitaxial growth using the seeded-beam SSJ involves a close collaboration between investigators at NCSU and Arizona State University (ASU). At ASU, the SSJ is interfaced directly into a low-energy electron microscope (LEEM) for the conduct of *in situ* studies of the nucleation and growth of epitaxial layers; while at NCSU, the SSJ systems are used to grow device-quality AlN, GaN and SiC for real applications. Exchanges in personnel (students) and information between the two groups ensures the achievement of desired results. The additional thin film growth experiments using dual-beam Colutrons and the theoretical studies referred to in this report are primarily conducted at ASU.

The research conducted in this reporting period and described in the following sections has been concerned with (1) preparation of 6H-SiC substrate surfaces, (2) theoretical modeling of atom/surface collisions and subsequent growth mechanisms, (3) design of new supersonic jet systems and ion beam technologies, and (4) deposition of GaN films via supersonic processes. The following individual sections detail the procedures, results, discussions of these results, conclusions and plans for future research. Each subsection is self-contained with its own figures, tables and references.

1. S. T. Ceyer, Langmuir **6**, 82 (1990).
2. S. T. Ceyer, Science **249**, 133 (1990).

II. Surface Morphology of Chemically Etched 6H-SiC(0001) Substrates for Thin Film Growth of III-V Nitrides

A. Introduction

For *in situ* real-time observation of growth of GaN and AlN layers in the low-energy electron microscope (LEEM), smooth substrate surfaces are required. However, the 6H-SiC(0001) wafers purchased from Cree Research have large networks of scratches due to mechanical polishing. The rough surface is not only detrimental to LEEM observations, which often precludes clear LEED patterns, but also gives rise to a large density of antiphase boundaries (APB) in the grown films propagating from the interface. In order to remove the scratches, etching and oxidation experiments of the 6H-SiC(0001) surfaces have been undertaken.

B. Experimental Procedure

For the etching experiments, a 50% by weight mixture of KOH and KNO_3 molten salts [1,2] was used. The 6H-SiC(0001) samples were individually immersed in the mixture at 600°C for durations ranging from 2.5 to 60 minutes. To smooth the substrate surface by oxidation, researchers took advantage of the fact that different crystallographic planes oxidize at different rates. After the formation of an SiO_2 layer with thickness in the range of 500–1000 Å, the oxide layer was removed by etching with a 1:10 H_2O:HF solution. The substrate surfaces were then examined by optical microscopy and scanning electron microscopy (SEM) before and after the etching and oxidation treatment.

C. Results and Discussion

Typical results are shown in the SEM micrographs of Figs. 1-3. As observed in Figs. 1-3, these treatments never completely succeeded in removing the scratches from the surface. However, it is interesting to note that the C-terminated $(000\bar{1})$ surface is consistently smoother than the Si-terminated (0001) surface. This result is reproducible on all the 6H-SiC samples that have a double-sided polish. The exact reason is unknown, but the more reactive nature of the C-terminated surface may play a role.

D. Conclusions

Removal of mechanical scratches from the 6H-SiC substrate surfaces by chemical etching and oxidation has not been completely successful although the C-terminated $(000\bar{1})$ surface appears to have a smoother finish. Such substrate surfaces can still present a problem for the growth of good quality epitaxial layers and for LEEM observations of growth.

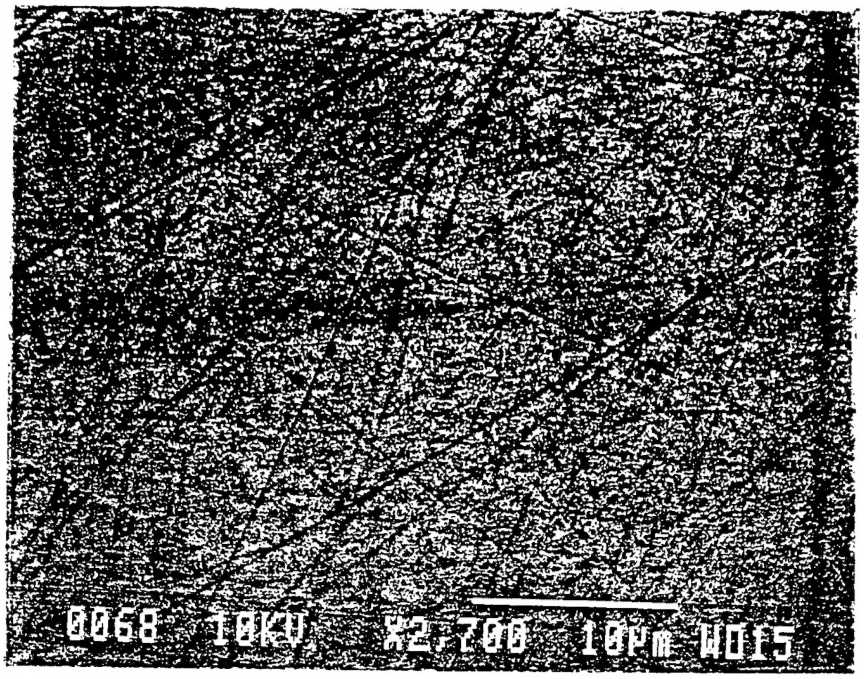

Si terminated, as received

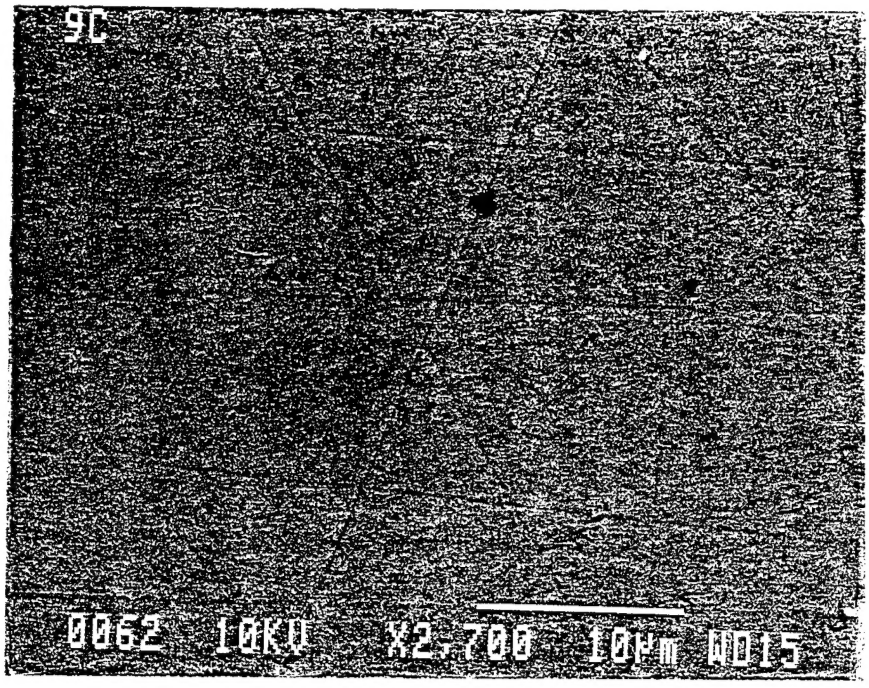

C terminated, as received

Figure 1. The as-received Si-terminated 6H-SiC(0001) and C-terminated (000$\bar{1}$) surfaces.

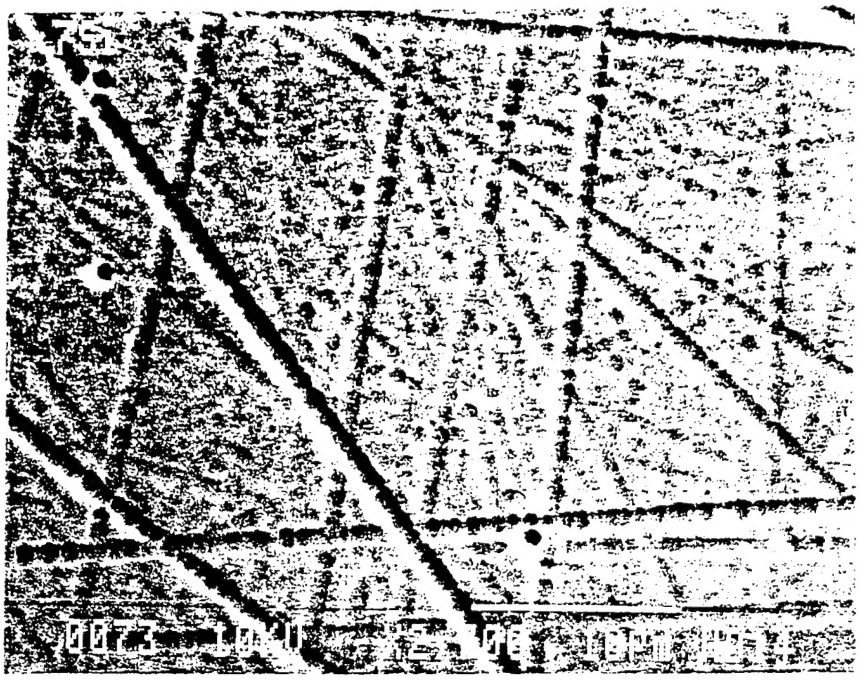

Si terminated, 5 minute etch

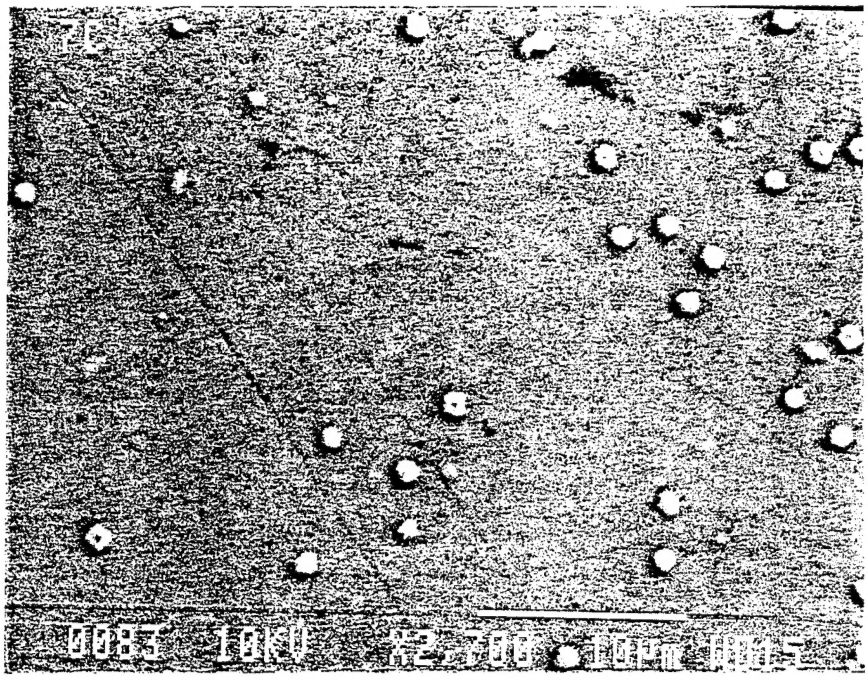

C terminated, 5 minute etch

Figure 2. The (0001) and (000$\bar{1}$) surfaces after 5 minutes of molten salt etch.

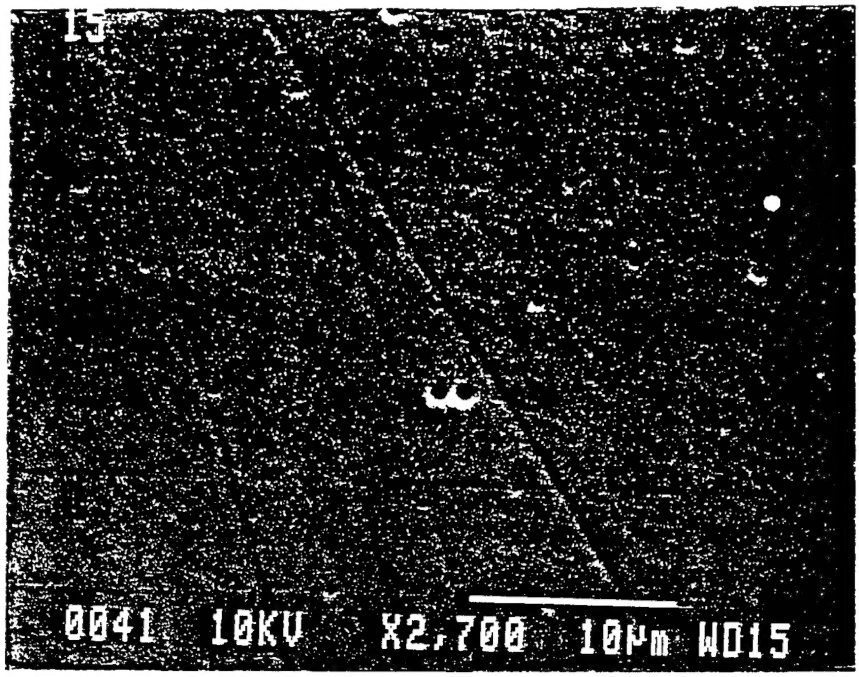

Si terminated, after oxidation

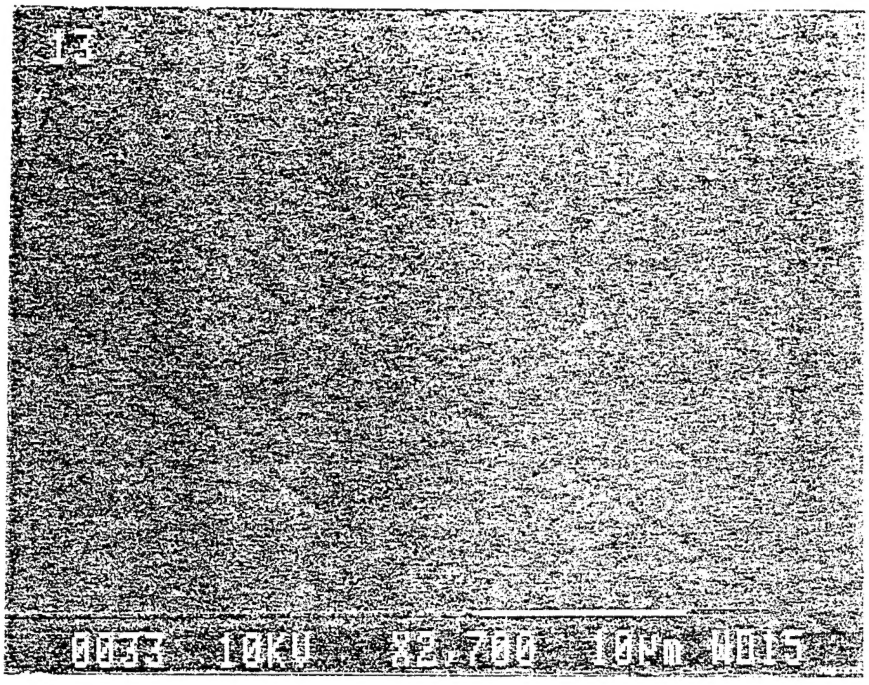

C terminated, after oxidation

Figure 3. The (0001) and (000$\bar{1}$) surfaces after oxidation and removal of the oxide layer.

E. Future Research Plans and Goals

We have informed Cree Research of the problems in the surface finish of their 6H-SiC wafers. Researchers from Siemens, Germany, with whom we have collaborations, appear to have developed a method to produce smooth flat surfaces of 6H-SiC(0001). The details of their method are proprietary. We intend to pursue further collaborations with the Siemens group to secure a steady supply of scratch-free substrates for our investigations.

F. References

1. R. W. Brander and A. L. Boughey, Brit. J. Appl. Phys. **18**, 905 (1967).
2. W. V. Muench and I. Peaffeneder, Thin Solid Films **31**, 39 (1976).

III. Theoretical Calculations of III-V Nitride Surfaces

A. Introduction

To understand the growth of the nitride compounds, we have undertaken two classes of calculations that correspond to two different time scales for the surface growth. The first calculations describe the collision dynamics of the neutral beam with the surface and the subsequent local incorporation and reconstruction of the surface. The initial goal of these calculations is to understand and quantify the barriers to surface bonding. These barriers determine the beam energy and angle that will be most effective for growing well-characterized surfaces. The calculations may also help us to identify optimal projectile compounds to use to seed the helium beam.

The second technique uses Monte Carlo methods to simulate the surface growth processes. This method will help us understand the growth kinetics on the time scales observed using the low energy electron microscope. Since these time scales are many orders of magnitude larger than the typical vibrational period of the optical phonons in the lattice (which set the scale of the time step needed in the molecular dynamics simulations), a first principles calculation is not possible. However, in the future, it may be possible to calculate the rates needed using quantum molecular dynamics.

B. Theoretical Methods

The calculations of the collision with and incorporation of atoms and molecules into the surface are being done using the localized orbital quantum molecular dynamics method developed by Sankey and Niklewski [1,2]. This method uses the adiabatic approximation to separate the nuclear and electronic motions. The electrons are always assumed to be in their ground state as the nuclei move. That is, the nuclear motion does not excite the many-body electronic states. The time evolution of the system is then given by solving Newton's equations for the nuclei [3],

$$\vec{F} = m\vec{a}, \tag{1}$$

where the nuclear potential is given by the residual nuclear coulomb interaction and the ground state energy of the electrons obtained by solving the many-body Schrödinger equation,

$$H\Psi = E\Psi. \tag{2}$$

While the ground state of atoms and molecules can be solved accurately for electronic systems of 20 or fewer electrons [4], these calculations are very time consuming. Since the

calculation of the nuclear trajectories can take thousands (or more) time steps, it is necessary that the solution of the Schrödinger equation be fast.

A variety of approximate methods can be used. These range from empirical tight-binding methods which can be very fast, but whose quality is dependent on how well the tight-binding Hamiltonian corresponds to the true physical situation. Since the parameters are not based on a fundamental energy or variational principle, it is easy to be led astray. A self-consistent plane wave local density approximation calculation can be done as in the Carr-Parinello approach. [5] The main problem is that the calculation can become quite large and time consuming.

In the Sankey-Niklewski approach, the electronic structure is solved with the following approximations: a local density approximation using the Harris energy functional is used [6]; the core electrons are replaced by a norm conserving pseudopotential the valence electronics states are expanded in localized orbitals, and the range of these orbitals is truncated by imposing a boundary condition on the Schrödinger equation that the single particle orbitals go to zero at a radius r_{cut}, dependent on the atomic species. The value of r_{cut} mimics some of the confinement effects of the solid, as well as introducing a cutoff into the overlap and Hamiltonian matrices so that these matrices can be more easily diagonalized. The Harris approach allows the electronic energy to be calculated without iterating the electronic density to self-consistency. However, we have included charge transfer effects into these calculations and the charge transfer is self-consistently calculated. Generally, the results are still quite accurate. The pseudopotential replaces the core electrons with an effective interaction, eliminating them from the calculation, leaving just the chemically important valence electrons. The localized basis allows us to calculate the local density orbitals by diagonalizing relatively small (typically 4N by 4N where N is the number of atoms) matrices. The electronic energy is calculated and its gradient with respect to the nuclear positions gives the forces which are used in the molecular dynamics method.

In addition, we are beginning some transport Monte Carlo methods to simulate the surface growth of GaN. In these calculations, we input Ga and N fluxes and sticking probabilities. The Ga and N atoms can then diffuse on the surface until they incorporate into the GaN lattice. Incorporated Ga and N atoms can evaporate to diffuse on the surface. The rates for all of these processes are modeled with simple Ahrenius temperature dependencies. The constants in these rates are selected from experiments or from our best estimates derived from other materials. Eventually, we want to calculate these rates using the quantum molecular dynamics or related method.

C. Results

We have begun by looking at the chemisorption of NH_3 on the Si(111) surface. We have two reasons for choosing this system. First, we need to know the energy barriers to

chemisorption encountered by nitrogen complexes that we plan to accelerate in the He beam. NH_3 is an obvious choice for a simple nitrogen compound. Second, we wish to test our calculations against the experimental results (and proposed model) of Tanaka *et al.* [7] for the behavior of NH_2 and NH_3 on the Si(111) surface. An added advantage is that these systems have only three species, so that the computations needed to calculate and store the needed three-center integrals are reduced from our later calculations which will need five species, for example, Ga, N, H, Si, C.

We have completed the calculation of the basis orbitals and the needed two- and three-center integrals. Some initial calculations have looked at NH_3 and H_2 to make sure that these molecules are reasonably well characterized with the orbital cutoff radii r_{cut} appropriate to the solid. The calculations were performed by simply "annealing" the molecules, so that the constituent atoms found their lowest energy conformation, using the quantum molecular dynamics method. For H_2, the calculated bond length is 0.7698 Å, in good agreement with the experimental value of 0.762 Å. For NH_3, the calculated HNH bond angle is 109.6°, compared to 107° experimentally. The bond length is 1.17 Å compared to the experimental values of 1.014 Å.

We are now calculating the NH_2 and NH_3 on Si(111). These calculations are initially set up using six layers of Si atoms in a 2×2 periodic system. The lowest layer of the Si atoms is given a very large mass and hydrogen terminated to model the effect of bulk Si. Initial calculations are being done by assigning the N atom a large mass and mapping out the potential energy surface of the NH_3 molecule as the N atom is brought close to the Si surface. We should complete the modeling of the region where the third H atom leaves the NH_3 and NH_2 incorporates on the surface soon.

D. Discussion

For the H_2 molecule, agreement with experiment is quite good as expected. The NH_3 molecule is less well characterized using the local density method. Part of this is due to the cutoff used for the H atom orbital. Since the H atoms are typically incorporated only at the surface to tie off dangling bonds, or in the projectile molecules, it may be possible to improve these results, by changing the r_{cut} value for hydrogen, without adding any additional errors to the calculations. In any case, the binding energies of the H atoms and the molecular conformation of the NH_3 molecule is still within about five percent, so we expect that the calculation of the energy barriers will be accurate enough to guide the experiments.

E. Conclusions

The quantum molecular dynamics calculations should be accurate enough to characterize short time incorporation of Al, Ga, and nitride compounds into the growing surface. The energy barriers should be calculated at least at a qualitative level. One of the problems with

quantitative calculation of these barriers will be the effect of excited many-electron states in the formation of the surface from the molecular bombardment. Since the quantum molecular dynamics method (like most dynamical methods) uses the adiabatic approximation, the electrons are always in their ground state. If the surface interaction causes a transition to an excited electronic state (an excited potential surface in the language of chemistry), the adiabatic approximation breaks down. Methods that can deal accurately with these transitions are not well developed. However, these transitions are most likely to occur when there are electronic degeneracies, and these can be monitored within our calculations.

F. Future Research Plans and Goals

A number of theoretical projects are planned although these may change as the needs of the experimental work change. We first plan to complete the characterization of the NH_3 on Si(111). Refinements to this work include adding a "thermostat" to the last row of Si atoms to model a heat bath from the bulk. We plan to investigate the role of charge transfer in the surface reconstruction.

The calculation of the orbitals and two- and three-center orbitals for more species is also planned. The electronic structure calculations have all been done using the IBM SP2 computer at the Cornell Theory Center. This machine currently has 512 processors in a fast message-passing architecture. Some of these processors have two Gbytes of memory. This should allow us to scale our current calculations up to calculations using five or more atomic species so that more complicated states of the surface can be investigated. The conversion of the present quantum molecular dynamics code to a parallel code has begun.

One long-range goal is to better understand and characterize the creation of nitrogen vacancies from a first principles point-of-view to allow us to devise methods that can produce high-quality films.

G. References

1. O. F. Sankey and D. J. Niklewski, Phys. Rev. B**40**, 3979 (1989).
2. O. F. Sankey, D. J. Niklewski, D. A. Drabold, and J. D. Dow, Phys. Rev. B**41**, 12750 (1990).
3. M. P. Allen and D. J. Tildesley, *Computer Simulation of Liquids*, (Oxford, London, (1987).
4. R. Subramaniam, M. A. Lee, K. E. Schmidt, J. W. Moskowitz, J. Chem. Phys. **97**, 2600 (1992).
5. R. Carr and M. Parinello, Phys. Rev. Lett. **55**, 2471 (1985).
6. J. Harris, Phys. Rev. B**31**, 1770 (1985).
7. S. Tanaka, M. Onchi and M. Nishijima, Surf. Sci. Lett. **191**, L756 (1987).

IV. Design of a Supersonic Molecular Beam Source for *In Situ* Growth of AlN and GaN Layers Observed by Low Energy Electron Microscopy (LEEM)

A. Introduction

The nitride family of AlN, GaN and InN thin films have shown to be strong candidates for electronic and optoelectronic applications. With direct band gaps of 6.2 eV, 3.4 eV and 1.9 eV for AlN, GaN and InN, respectively, solid solutions based on these materials provide for band gap modifications suitable for applications ranging from the red to the deep UV region of the spectrum [1]. However, the growth of single crystal, epitaxial films with low defect densities has proven to be troublesome. As-deposited GaN shows n-type behavior. It has been proposed that this n-type behavior is due to N vacancies [2]. These vacancies are formed during growth due to the high temperature required to decompose N sources such as NH_3 and to obtain high enough surface mobilities such that a single crystal film is achieved. N sources such as cold cathode ion guns [3] and microwave discharges [4-5] have been used to dissociate N_2 and N_2/NH_3 mixtures, respectively, and allow low temperature (i.e. 650°C) growth of GaN. However, it has been shown that high temperature anneals will improve the carrier density and crystallinity of the films [6]. Therefore, a technique which would provide a N source with a low decomposition temperature and high surface mobility is required to overcome these difficulties.

Supersonic Molecular Beam Epitaxy (SMBE) has been shown to enhance the surface decomposition of silane and methane [7,8]. This is due to the possibility of tuning the kinetic energy of these species such that bond cleavage and deformation occurs upon contact with the substrate. If the kinetic energy available is higher than the barrier for chemisorption on these surfaces, some of the remaining energy can be used to enhance surface diffusion via the generation of surface phonons or the use of surface kinetic energy by part of the adsorbate. SMBE also provides for the tuning of the energy spreads. This is important in order to experimentally determine the chemisorption barriers for the systems being studied, as well as to provide species with high sticking coefficients at high enough intensities. SMBE is, therefore, a suitable technique for the growth of single crystal GaN films at suitable growth rates. A review of supersonic molecular beams can be found in Scoles [8].

The present report entails the design and construction of a supersonic molecular beam source to be interfaced with the Low Energy Electron Microscope at Arizona State University. This will allow for the study of the growth mechanisms, as well as defect evolution during the deposition of GaN and AlN. The ability of such *in situ* analysis will further the development of these films by providing instant feedback on the atomic processes involved during the deposition of these films.

B. Experimental Procedure

Geometric constraints were the main issue for the chamber design. The geometry was dictated mainly by the LEEM which is shown in Fig. 1. The SMBE source will be interfaced using a side 2 3/4" CF port which makes a 72° angle with the surface normal of the substrate or a port normal to the sample surface. If the total energy of the reactant is effective in promoting dissociative chemisorption, the 72° port will be used since it would not require chopping the beam. If however, the incident kinetic energy relative to the surface normal proves to be the main activation path, the port normal to the substrate will be used. Using this port would require chopping the SMBE and LEEM beams out of phase such that the reactants are not ionized by the electrons in the LEEM. The SMBE chamber requires high stagnation pressures to obtain narrow energy distributions and high intensities. Because the LEEM requires the chamber pressure to be less than 1E-7 torr, two differential pumping stages were designed to decrease the gas load and collimate the beams. The finalized chamber design is shown in Figs. 2(a),(b) and (c).

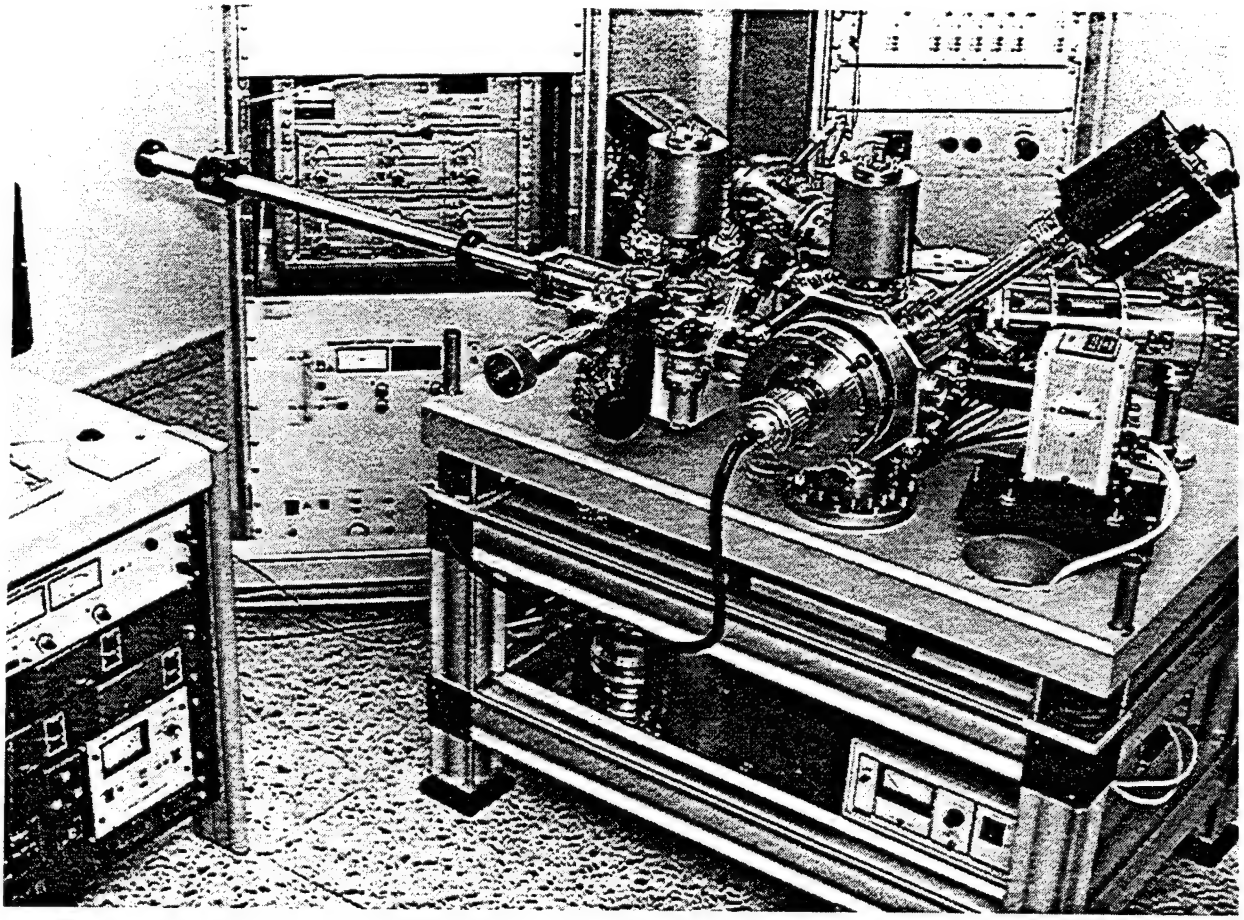

Figure 1. Low energy electron microscope at Arizona State University.

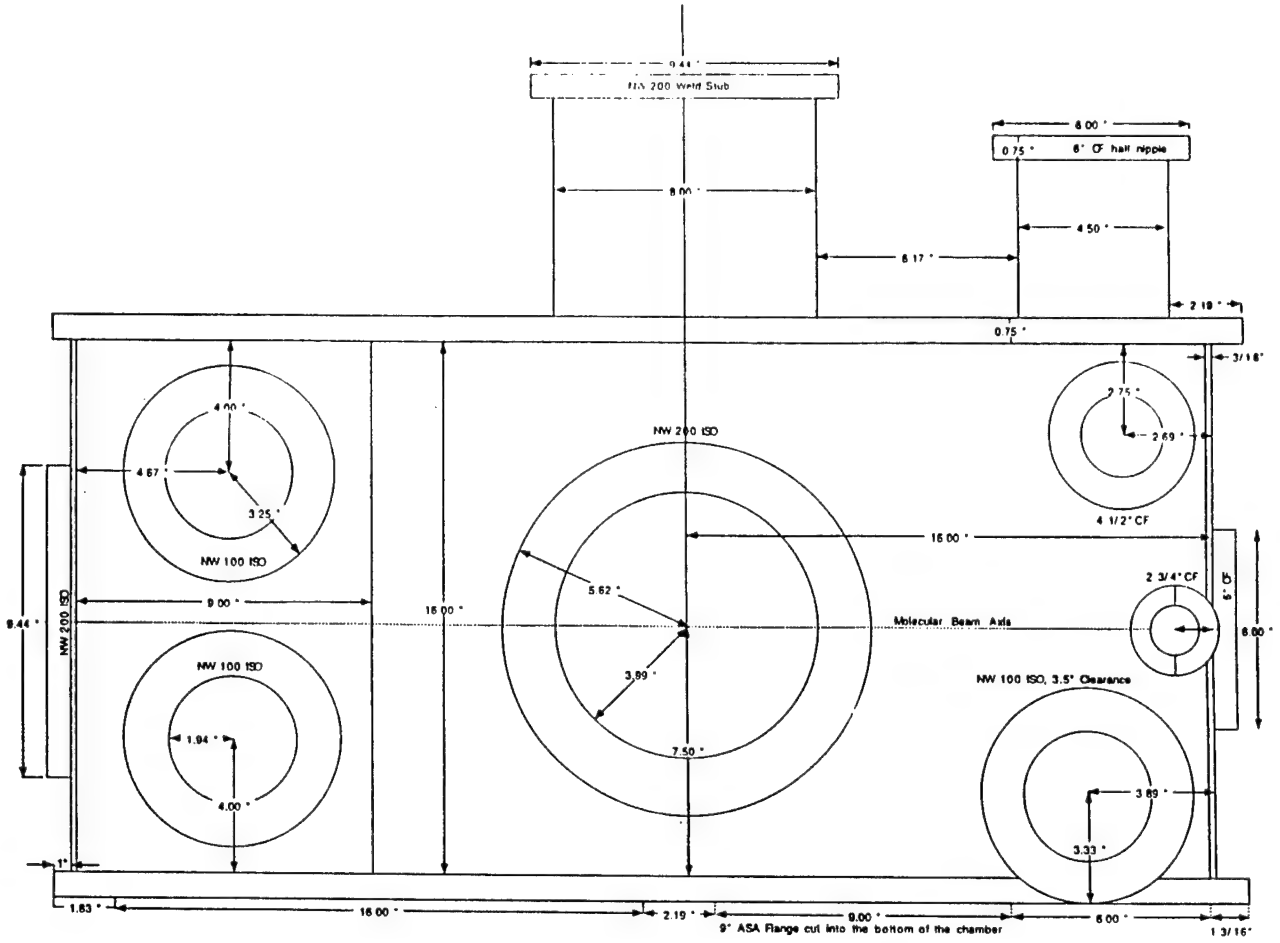

Figure 2(a). Right side view of the SMBE chamber.

The pump selection was based on geometry suitable for interfacing the SMBE source with the LEEM. The source sub chamber will be pumped by a Varian VHS-10 diffusion pump which will be backed by a combination of a Leybold WSU 501 Roots Blower and a Leybold D65-BCS rotary vane pump. This will allow a maximum throughput of 7.7 torr l/s. The ideal pressure in this chamber will be 0.5–1.0 mtorr. The roots blower will allow us to work at pressures higher than these. The first differential pumping stage will be pumped by a Varian VHS 4 diffusion pump with a Varian 362-4 cryotrap. This will allow the pressure in that chamber to be 5E-6 to 1E-5 torr. The second differential pumping stage will be pumped by a Leybold TMP 340M magnetically suspended turbo pump. The pressure in this chamber will be 5E-8 to 1E-7 torr during operation. This combination of pumps provided the highest throughput possible for the design constraints involved.

Aligning the beam and the skimmer to optimize intensity and energy distributions will be done by using a manipulator mounted vertically onto the chamber and it provides for x-y-z

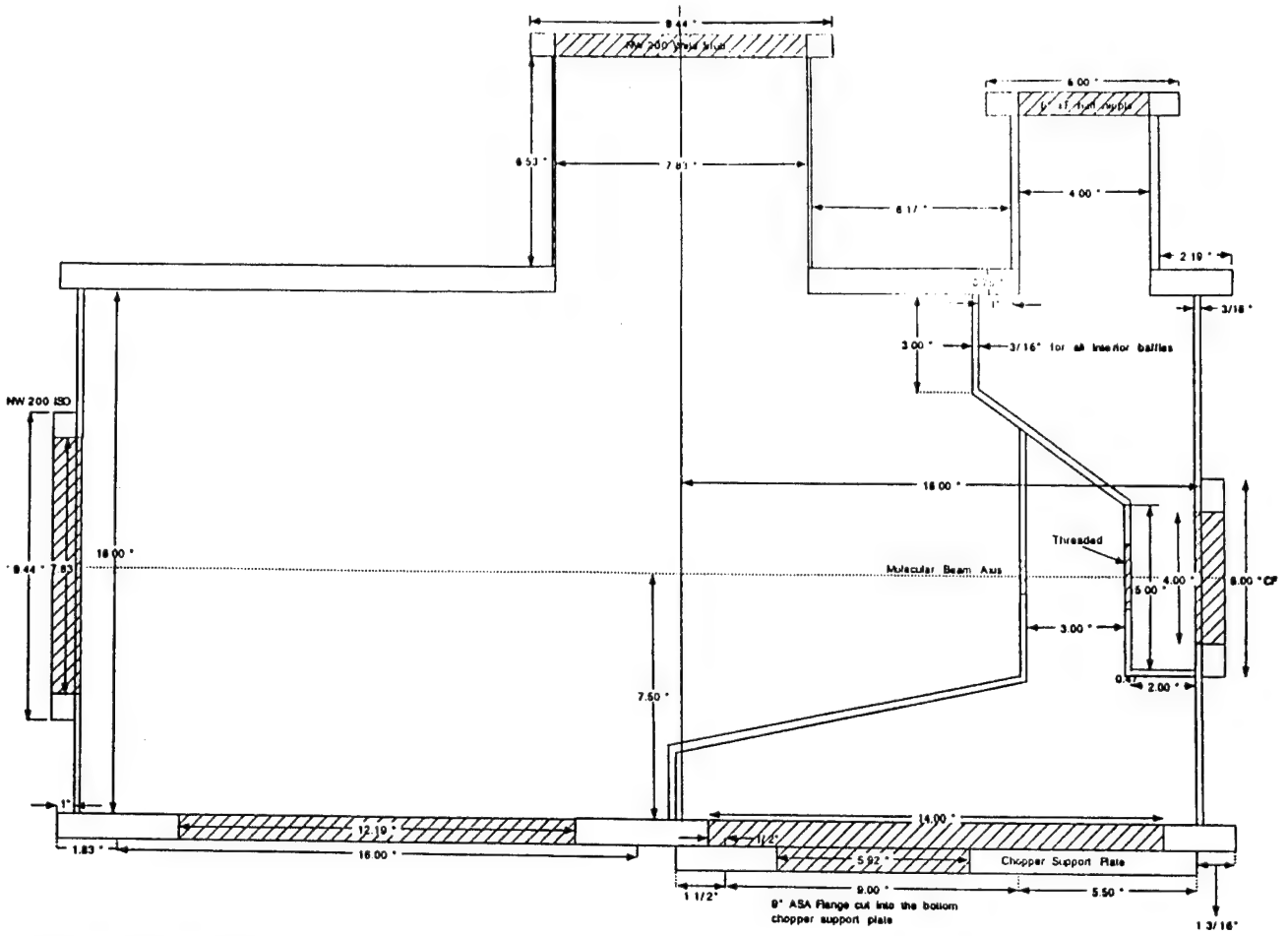

Figure 2(b). Right side cross-sectional view of the SMBE chamber (note internal partitions).

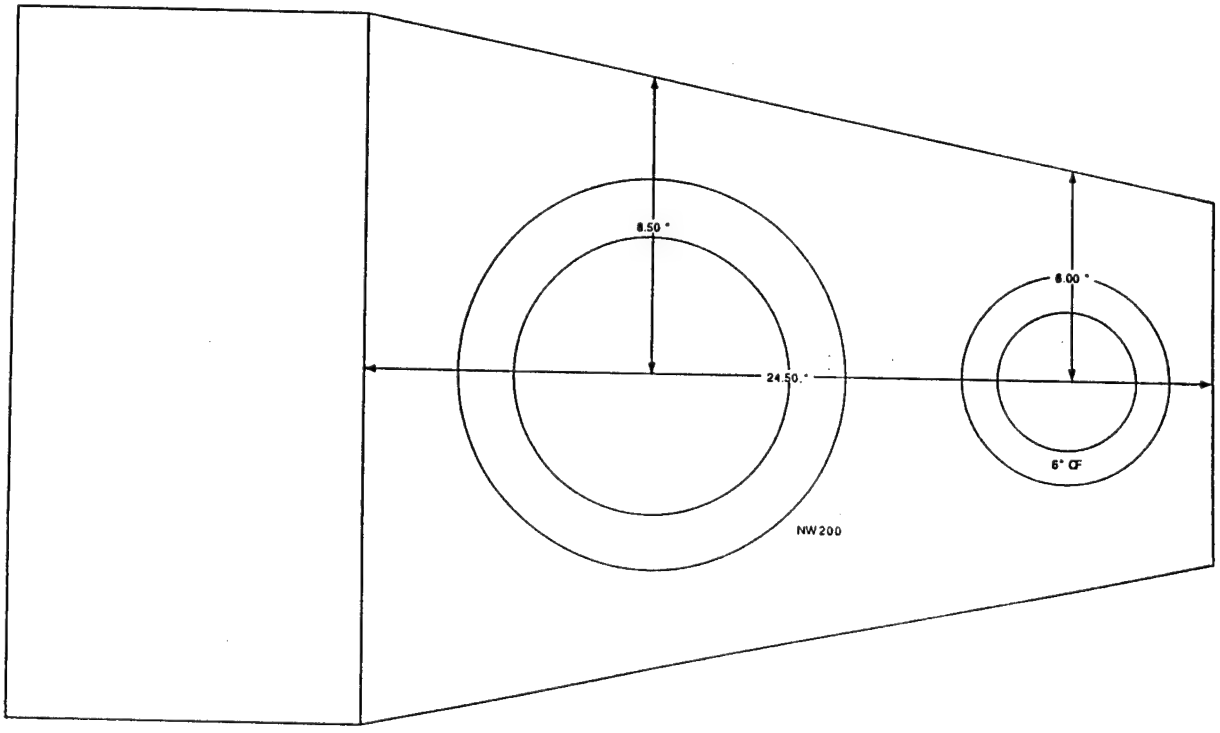

Figure 2(c). Top view of the SMBE chamber.

movement of the nozzle. The nozzle consists of a 1/4" O.D. stainless steel tube with a screw-on cap which holds apertures of various sizes. This design allows for the use of pressures exceeding 1000 PSI. These high pressures are necessary in order to control the energy spreads of the beams.

The gas handling manifold was designed using the throughput of the pumps as a limitation. Eq. 1 relates the pump throughput (T), to the reservoir pressure (P_o), reservoir temperature (T_o) and nozzle diameter (d):

$$T = C(T_c/T_o)(300/T_o)^{0.5}(P_o d^2), \quad (1)$$

where C is a gas composition dependent constant and T_c is the chamber temperature. The mass flow (m) through the nozzle can be expressed as:

$$m = P_o A((\Omega W/RT_o)(2/(\Omega+1))^{(\Omega+1)/(\Omega-1)})^{0.5}, \quad (2)$$

where A is the nozzle area, R is the universal gas constant, W is the molecular weight of the expanded gas and Ω is the ratio of the heat capacities at constant pressure and constant volume. By balancing these two equations a maximum flow rate of 1000 sccm of total gas was calculated. The selection of mass flow controllers was dictated by this total throughput and the gas composition.

To obtain a wide range of P_o, the gasses (NH_3 and He) will be premixed and fed to a two-stage, air-driven diaphragm compressor to obtain reservoir pressures as high as 2000 PSI. By using a 146 MKS cluster gauge controller, the suction pressure as well as the flow through the compressor will be controlled by MFCs as shown in Fig. 3. The need for a high nozzle pressure is due to the fact that the energy spread scales with the product of the nozzle pressure (P_o) and nozzle diameter (d). However, because $P_o d^2$ is fixed by the throughput of the pumps, increasing $P_o d$ implies decreasing d and increasing P_o. Decreasing d must be done with care so as not too cause the orifice to clog up. The current design would allow values of $P_o d$ up to 50 torr-cm. However, the maximum nozzle pressure at a given temperature should be chosen such that condensation does not occur. Therefore, beam composition is a factor in $P_o d$.

C. Results

The modeling of beam characteristics is necessary to establish the experimental parameters such as reservoir pressure, reservoir temperature and gas composition which control the intensity, energy and energy spread. The average beam velocity for each component (u_i) is mainly controlled by the reservoir temperature, gas composition and beam temperature for each component (T_i) via:

$$u_i = (2\Omega_c kT_o/((\Omega_c-1)m))(1-(T_i/T_o))^{0.5}, \quad (3)$$

where m is the average mass of the gas mixture. The main variable to be solved to model the average velocity and, therefore, energy of the beam is the beam temperature. Miller [9] provides a model for determining the beam temperature for each species of binary monoatomic gasses.

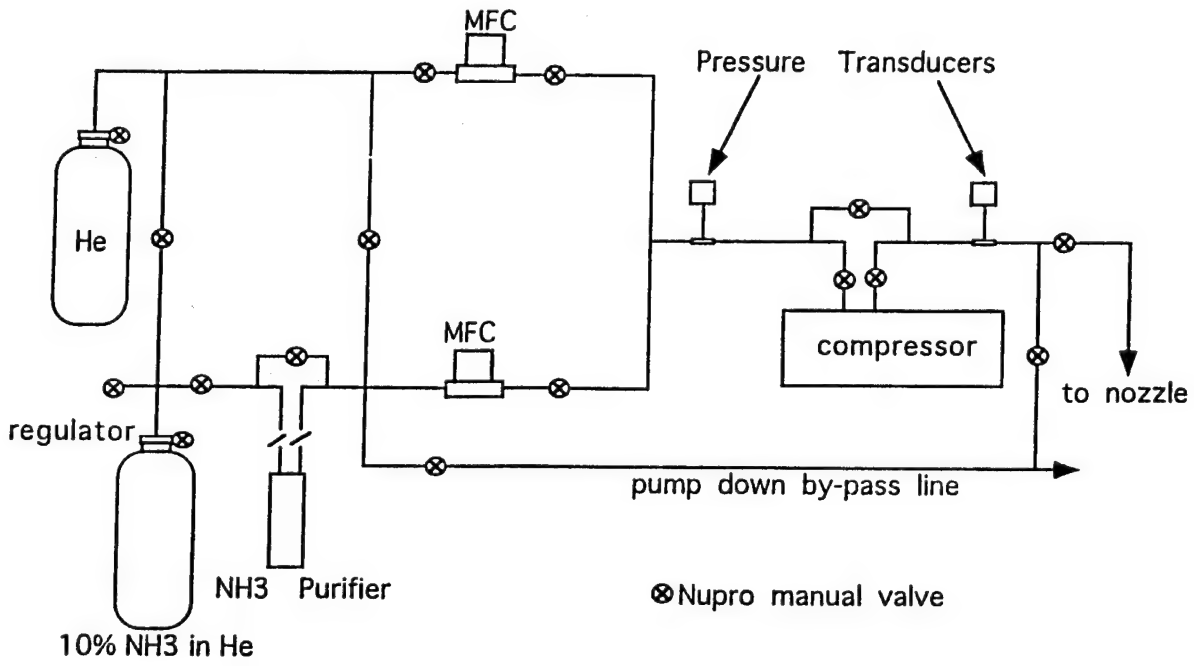

Figure 3. Gas manifold for the SMBE chamber.

Since NH_3 is not monoatomic and rotational, as well as vibronic, modes might contribute to the beam temperature. However, these will be ignored since they are not accountable by any available model. The current model might give some reasonable idea of the beam properties if the flow is such that a rescaling to monoatomic gasses can be done at the point where the internal degrees of freedom freeze [9]. This assumption holds fairly well at low temperature where the vibrational and rotational modes are in the ground state. T_l (beam temperature for the light species) and T_h (beam temperature for the heavy species) are related to the stagnation temperature via:

$$T_l = T_o(TSP_l)^{-1.064} \tag{4}$$

$$T_h = T_o(TSP_h)^{-1.112} \tag{5}$$

where TSP is the Temperature Slip Parameter. The TSP can be calculated using the following equation:

$$TSP_i = C_i n_o d(m/\mu_{ij})^{0.5} \quad (6)$$

where n_o is the reservoir number density which is proportional to the reservoir pressure, d is the nozzle diameter, m is the average mass of the mixture and μ_{ij} is the reduced mass. C_i is a complex function which depends on gas composition and the collision cross sections of the individual components. The collision cross section for NH_3 was calculated using the interatomic potential for $(NH_3)_2$ [10]. The He hard sphere scattering cross section was used since the potential well for this system is much lower than the kinetic energy [9].

Once the above has been solved and assuming that the velocity distribution $g(v_i)$ remains as that of a Gaussian, $g(v_i)$ can be expressed as:

$$g(v_i) = Nv^2 \exp(-(m_i/2kT_i)(v-u_i)^2),$$

where N is a normalization constant and k is Boltzmann's constant [11].

D. Discussion

This model was used to predict the behavior of the velocity distributions under various source conditions. Figures 4(a) and 4(b) show the velocity distributions calculated for He and NH_3 beams. As expected for pure beams, the mean velocity of the gas scales with the mass. The velocity spread (full width at half max.) is larger for He than for NH_3 due to a smaller collision cross section.

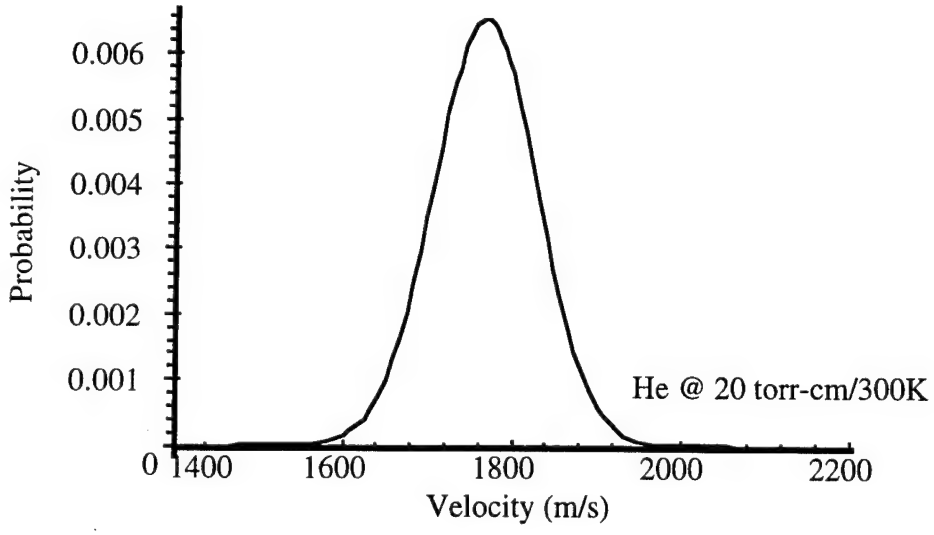

Figure 4(a). Pure He beam at 20 torr-cm / 300K.

Figure 5 shows the velocity distribution for a NH_3 for a 6% NH_3 in He molecular beam at 20 torr-cm and 300K. The average velocity of the beam increases due to the seeding effect.

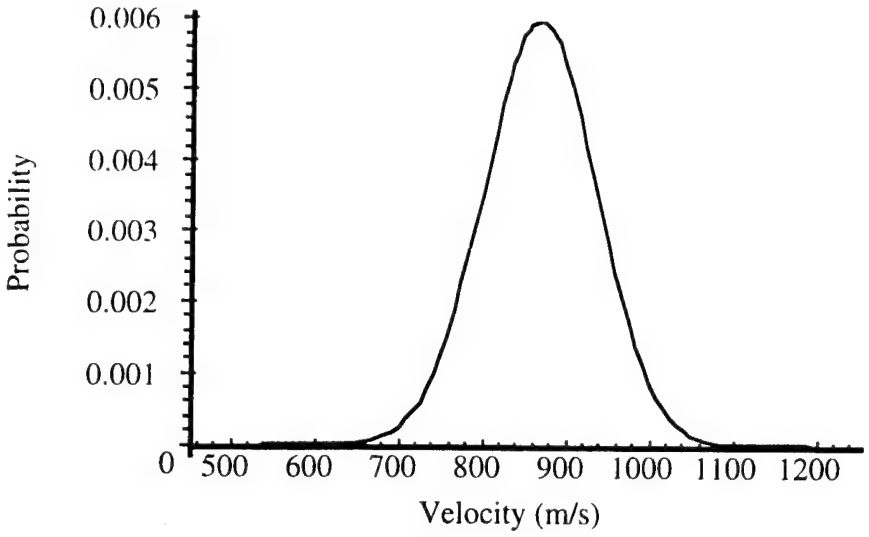

Figure 4(b). Pure NH_3 beam at 20 torr-cm / 300K.

However, the velocity spread has increased due to the compositional dependence of C_i and the increase in average velocity. If the amount of NH_3 is decreased the velocity distribution would shift toward that of pure He. Therefore, controlling the gas composition provides a means of controlling kinetic energy, as well as energy spread.

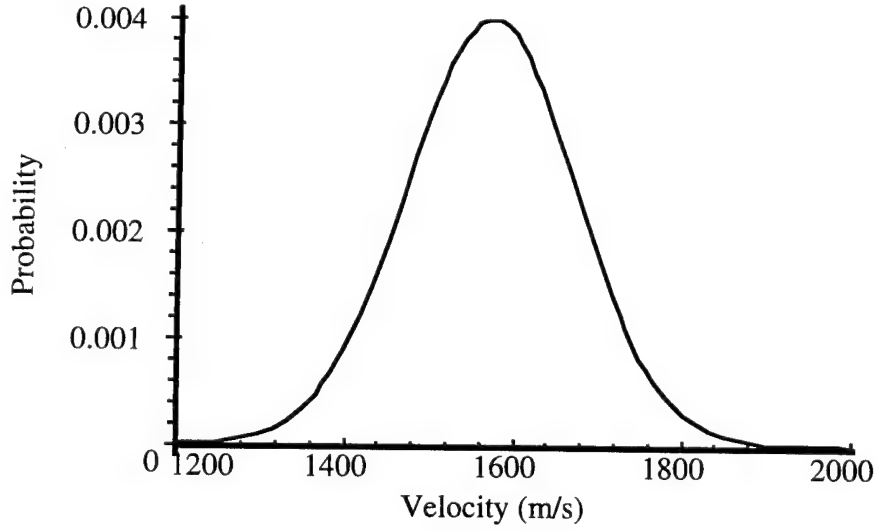

Figure 5. 6% NH_3 in He at 20 torr-cm and 300K.

Figure 6 shows the calculated velocity distribution for a 6% NH_3 in He beam at 20 torr-cm and 600K. The mean velocity of the beam increased to 2147 m/s. There is an increase in the velocity spread due to the increase in T_o. At higher temperatures, the velocity spread might increase further if there are contributions from the vibrational and rotational motions to the scattering cross section.

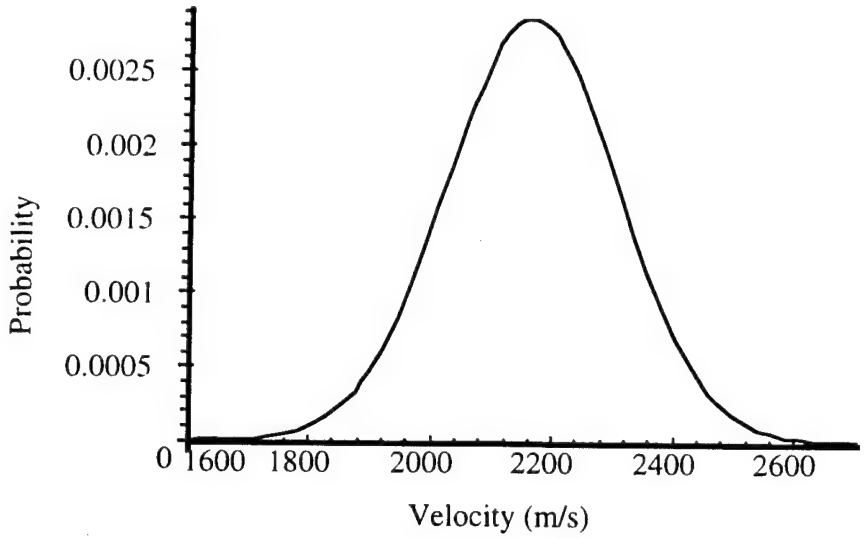

Figure 6. 6% NH_3 in He at 20 torr-cm and 600K.

Figure 7 shows a calculated velocity distribution for NH_3 in a 6%NH_3 in He beam at 30 torr-cm and 300K. The decrease in velocity spread is due to the increase in P_od.

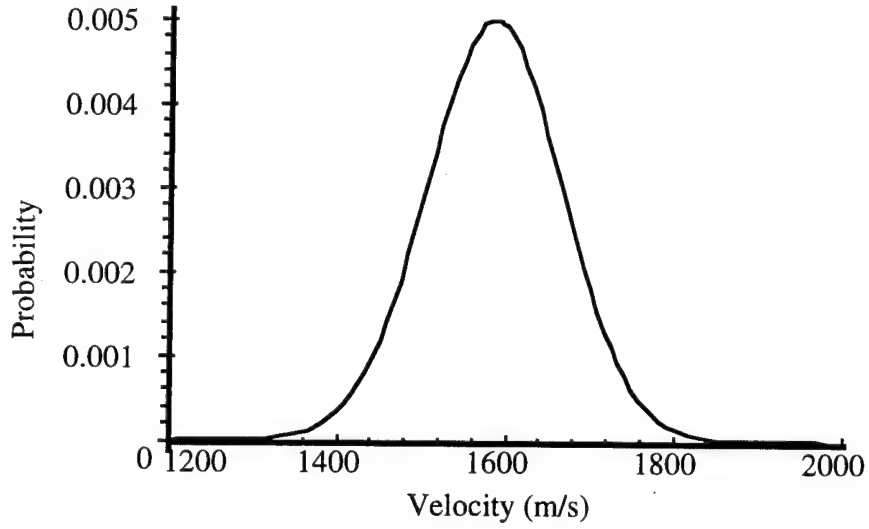

Figure 7. 6% NH_3 in He at 30 torr-cm and 300K.

The calculations used would predict beam characteristics which are in reasonable agreement with those experimental results obtained by R. B. Kay (12) for 6% NH_3 in H_2 beams. Therefore, the assumptions made to justify the use of the binary monoatomic model, seem to be reasonable.

In the context of film deposition using NH_3, it is important to use beams of appropriate energy in order to induce low temperature decomposition. If the energy spread of the beam lies

above the minimum energy required to see this "translationally activated dissociation," the efficiency of the process would increase and higher growth rates would be predicted. However, for epitaxial single crystalline films the growth rate has to be such that a layer by layer or 2D growth mode is induced. The growth rate is a function of beam composition (i.e. number of NH_3 molecules directed toward the surface), mean kinetic energy and energy spread. Theoretically the optimization of the beam energy and energy spread would lead to a decrease in by products because of the elimination of gas phase reactions at low temperature and the more efficient use of the reactants would allow for growth at lower pressures.

E. Conclusions

The design of a SMBE source chamber with two differential pumping stages to be interfaced with the LEEM has been shown. A gas manifold capable of producing beams with a reasonable energy and energy spread has been designed to feed gas into the system. P_od values as high as 50 torr-cm will be achieved with this design. The characteristics of supersonic NH_3/He beams have been predicted using the monoatomic binary gas approximation. As shown the use of supersonic beams provides for control of kinetic energy, as well as energy spread. Optimization of these beam characteristics would lead to efficient film growth at reasonable rates. N and dopant incorporation problems can be overcome by this technique.

F. Future Research Plans

The gas manifold will be tested in the Helium Atom Scattering (HAS) chamber and NH_3/He beams will be characterized at a range of gas compositions, T_o and P_od. The SMBE chamber will be finalized and tested with the proposed gas manifold. GaN LEEM studies using SMBE will be performed once deposition has been achieved in the HAS chamber and a preliminary set of growth parameters have been identified. The initial attempt will involve evaporated Ga and Al, and high kinetic energy NH_3.

G. References

1. S. Strite, H. Morkoc, J. Vac. Sci. Technol. B. **10**(4), (1992).
2. A. Estes Wickenden, D. K. Wickenden, T. J. Kistenmacher, J. Appl. Phys. **75**(10), (1994).
3. Z. Q. He, X. M. Ding, X. Y. Hou, Xun Wang, Appl. Phys. Lett. **64**(3), (1994).
4. M. J. Paisley, Z. Sitar, J. B. Posthill, R. F. Davis, J. Vac. Sci. Technol. A, **7**(3), (1994).
5. H. Okumura, S. Misawa, T. Okahisa, S. Yoshida, J. Cryst. Growth **136**, 361, (1994).
6. D. K. Wickenden, J. A. Miragliotta, W. A. Bryden, T. J. Kistenmacher, J. Appl. Phys. **75**(11), 7585, (1994).
7. M. E. Jones, L. Q. Xia, N. Maity, J. R. Engstrom, Chem. Phys. Lett. **229**, 401, (1994).
8. S. T. Ceyer, J. D. Beckerle, M. B. Lee, S. L. Tang, Q. Y. Yang, M. A. Hines, J. Vac. Sci. Technol. A **5**(4), (1987).

9. D. R. Miller, A*tomic and Molecular Beam Methods*, Ch. 2, Ed. G. Scoles, 1988, Oxford University Press.
10. G. Duquette, T. H. Ellis, G. Scoles, R. O. Watts, M. L. Klein, J. Chem. Phys. **68**(6), (1978).
11. S. DePaul, D. Pullman, B. Friedrich, J. Phys. Chem. **97**, 2167, (1993).
12. R. B. Kay, private communication.

V. Design of Dual Colutron Ion Beam System for Deposition of SiC and GaN

A. Introduction

The goal of this work is to produce crystalline SiC and GaN films by depositing the chemical components by two ion beams simultaneously. The ion sources are each equipped with a Wien filter to select the mass of the ions. By using electrostatic deceleration lenses, the ion energy can be selected in the 10 eV range with an energy spread as low as 0.1 eV.

The growth process is monitored during the ion deposition by a Reflection High-Energy Electron Diffraction (RHEED) system. A retarding field analyzer is used to examine the structure and composition of the deposited films *in situ* by low-energy electron diffraction (LEED) and Auger Electron Spectroscopy (AES).

B. Experimental Procedure

In the first phase of the project, the ion beam deposition chamber was designed. The vacuum system consists of three separate compartments. The main chamber is connected to two Colutron ion sources which are pumped separately. The ion deceleration lenses are mounted inside the chamber, as close to the sample surface as possible. In our design, a distance of 3 cm between the sample surface and the exit of the deceleration lenses and an angle of 15° between the ion-beam direction and the surface normal are maintained. Inside the chamber, a electrostatic hemispherical sector energy analyzer is mounted on a turntable. This analyzer facilitates the measurements of energies of ions from both ion sources by positioning the analyzer directly opposite to the exit lens of the decelerators. To characterize the ion beams, a Faraday cup is mounted at the end of the sample manipulator. This cup has a small, well-defined entrance aperture and enables both determinations of the ion beam profile and the current density at the sample location.

A RHEED system is aligned parallel to the sample surface, with the electron gun and fluorescent screen in opposite directions. The axis of the screen has an offset of 15.2 mm to the electron gun axis in order to use a larger screen area for the diffraction image. For films growing layer-by-layer, RHEED is a simple method to determine the film thickness in mono-layers by observing the intensity oscillations in the diffracted electron beams. By analyzing the diffraction pattern itself, a structural analysis of the grown film is possible [1-4].

The manipulator is designed to enable sample heating by a direct current through the sample. The sample temperature between 300 and 1200°C is measured by a infrared pyrometer outside the chamber via a CaF_2 viewport.

The samples are loaded into the main chamber through a load lock chamber which is separately pumped. Another transfer mechanism enables the use of a retarding field analyzer in

a separately pumped third chamber to perform *in situ* LEED and AES analysis of the deposited films.

All chambers of the vacuum systems are equipped with viewports for the control of the transfer process and with ionization gauges for total pressure measurements. The main chamber is additionally equipped with a quadrupole mass spectrometer to perform residual gas analysis.

C. Results

The design of the chambers as described above has been completed. The vacuum chambers are under construction. The Colutron ion beam systems have been assembled. New sources for the production of the different ion beams have been purchased. In addition, the RHEED system was purchased and delivered. Other components for the vacuum systems were taken from existing UHV systems, checked and serviced, when necessary.

D. Future Research Plans and Goals

The vacuum system will be assembled upon the arrival of the chambers. As a first step, Si and C ion beams will be generated and characterized. SiC films will be produced on SiC substrates. In a second step, the ion sources will be converted to Ga and N ion beams to produce GaN films on SiC substrates.

E. References

1. J. J. Harris, B. A. Joyce, P. J. Dobson, Surface Sci. **103**, L90 (1981).
2. J. M. Van Hove, C. S. Lent, P. R. Pukite, P. I. Cohen, J. Vac. Sci. Technol. **B 1**, 741 (1983).
3. J. H. Neave, B. A. Joyce, P. J. Dobson, N. Norton, Appl. Phys. **A 31**, 1 (1983).
4. J. E. Mahan, K. M. Geib, G. Y. Robson, R. G. Long, J. Vac. Sci. Technol. **A 8**, 3692 (1990).

VI. Deposition of GaN Thin Films Using Supersonic Jet Technology

A. Introduction

The potential optoelectronic applications of wide bandgap materials have stimulated considerable research concerned with thin film growth, characterization and device development of the III-V nitrides, namely cubic BN, AlN, GaN and InN. Of this family GaN has been the most thoroughly studied. Measures of the potential of GaN are revealed by the high Johnson's and Keye's figures of merit of 80.0×10^{11} and 4.2×10^{8}, respectively, compared to 4.75×10^{11} and 2.39×10^{8} for silicon[1]. Gallium nitride usually forms in the wurtzite structure with a bandgap of 3.4 eV[2]. However, several groups[3-6] have deposited films of the cubic (zincblende structure) β-GaN which has a smaller bandgap of 3.26 eV. As the wurtzitic polytype of GaN forms continuous solid solutions with both AlN and InN which have bandgaps of 6.2 eV[7] and 1.9 eV[8], respectively, materials having engineered bandgaps may be produced for the construction of optoelectronic devices that are active from the visible to the deep ultraviolet frequencies.

A major difficulty in the growth of thin films of GaN is the lack of suitable substrates. The lattice parameters and coefficients of thermal expansion are given in Table I for GaN and the most common substrate materials of Si, SiC (6H and 3C), sapphire, ZnO and GaAs. With the possible exception of the basal planes of α(6H)-SiC and ZnO, none of these materials are suitable for the two-dimensional epitaxial growth of GaN.

Table I. Physical Properties of GaN and Potential Substrate Materials[3]

Material	Lattice Parameter	Coefficient of Thermal Expansion
GaN	a = 3.189 Å	5.59×10^{-6} K^{-1}
	c = 5.185 Å	3.17×10^{-6} K^{-1}
Si	a = 5.43Å	3.59×10^{-6} K^{-1}
α-SiC (6H)	a = 3.08 Å	4.2×10^{-6} K^{-1}
	c = 15.12 Å	4.7×10^{-6} K^{-1}
β-SiC (3C)	a = 4.36 Å	2.7×10^{-6} K^{-1}
Al_2O_3	a = 4.758 Å	7.5×10^{-6} K^{-1}
	c = 12.991 Å	8.5×10^{-6} K^{-1}
GaAs	a = 5.653 Å	6.0×10^{-6} K^{-1}

To reduce thermal budgets and permit finer scale architecture, low GaN deposition temperatures are highly desirable. However, as deposition temperature is reduced, the surface mobility of deposition precursors is curtailed and film crystallinity and morphology are compromised. In addition to decreased surface mobility, another difficulty with low temperature GaN deposition is that the source materials, TEG and NH_3, decompose at greatly different temperatures. As the NH_3 molecule is more stable than the triethylgallium molecule, a mechanism to enhance the reactivity of ammonia is desirable.

Seeded supersonic beams may potentially drive the reaction and dissociative chemisorption of NH_3 on select substrates. By increasing the kinetic energy of the seeded molecules, a substantial amount energy can be carried by each molecule that can drive surface reactions when the molecule strikes the substrate surface. Engstrom *et al.*[10] have determined that the reaction probability of Si_2H_6 on the Si(100) increases rapidly for incident supersonic beam energies above about 23 kcal mol^{-1}. This effect may be applied to the reaction of NH_3 on selected substrate.

The objective of this research is to develop techniques for depositing GaN films using seeded supersonic jets. The immediate goal is to produce GaN films at reduced temperatures and determine the effect of varying deposition conditions on film character. Toward this end, GaN with an existing single jet system are being studied to determine ranges of growth parameters for GaN film deposition that can be used in a dual beam system now under construction.

B. Experimental Procedure

Sample Cleaning. Si(100) and Si(111) substrates were cleaned in a three step process: First the substrates were immersed in a 10% HF solution for 1 minute to remove the native oxide. Next, the samples were exposed in air to ultra violet light to oxidize the surface. After the illumination, the substrates were again immersed in the 10% HF solution prior to loading into the reactor.

Al_2O_3(0001) substrates were cleaned via a multiple step process. Firstly, the samples were successively ultrasonically cleaned in trichloroethylene, acetone and methanol. After water rinsing, the samples were immersed in a 70°C, 50:50 mixture of H_3PO_4 and H_2SO_4 for 5 minutes. After water rinsing, the substrates were finally immersed in a 10% HF solution immediately prior to installation in the reactor.

Deposition Reactor. A schematic of the single beam deposition system is presented in Fig. 1. This system may be operated in either of two modes depending on whether a skimmer is installed. All work up to this point has been conducted in the free jet mode where a skimmer is not installed.

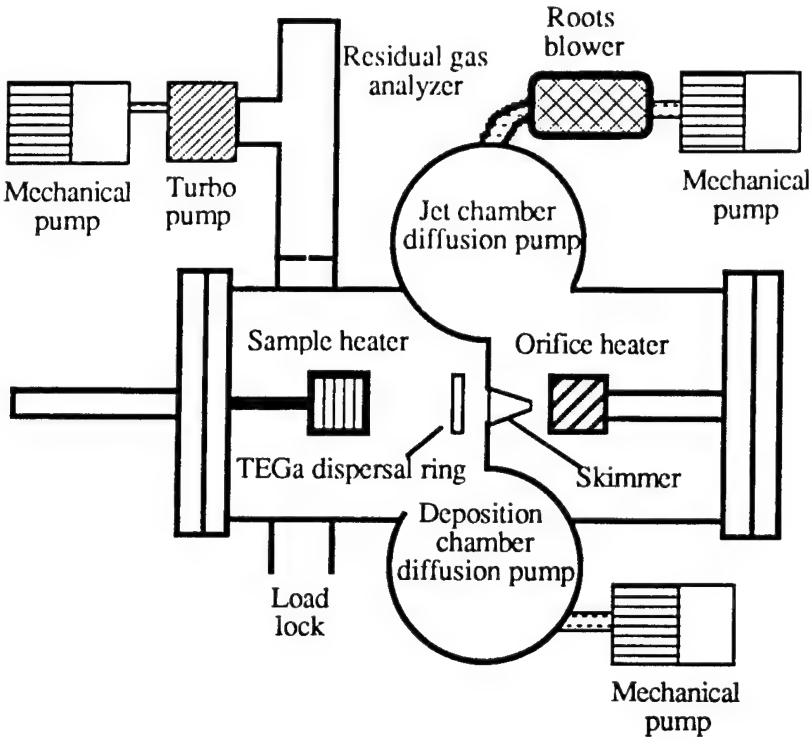

Figure 1. Single beam supersonic jet deposition system.

Deposition. After installation in the reactor, the samples are heated to the deposition temperature while a 5% NH_3 in He gas flow is maintained through the reactor. Typical deposition conditions are listed in Table II. As indicated in the table, although the total flow rates may vary, an NH_3 to TEG ratio of ≈200 has been found to produce the best films. After deposition, the TEGa flow is terminated and the sample is cooled to <200°C under flowing NH_3 /He.

Table II. Typical GaN Deposition Conditions

Parameter	Value
Substrate temperature	540° to 580°C
Orifice pressure	600 to 1000 Torr
Orifice temperature	510°C
Orifice gas	5% NH_3 in He
TEG bubbler temperature	-5 to 10°C
TEG bubbler pressure	800 Torr
TEG carrier	5 to 40 sccm He
NH_3/ TEG ratio	≈200

C. Results and Discussion

Film Deposition. Stoichiometric GaN films can be produced across the range of process variables listed in Table II. A scanning electron micrograph of a GaN film deposited on a Si(111) substrate is presented in Fig. 3. This film was deposited at 560°C and exhibited excellent thickness uniformity and minimal surface roughness. Figure 4 is a scanning electron micrograph of a GaN film deposited on an Al_2O_3(0001) substrate under conditions identical to those for the film in Fig. 3. This latter film was not of uniform thickness and has a much more irregular surface.

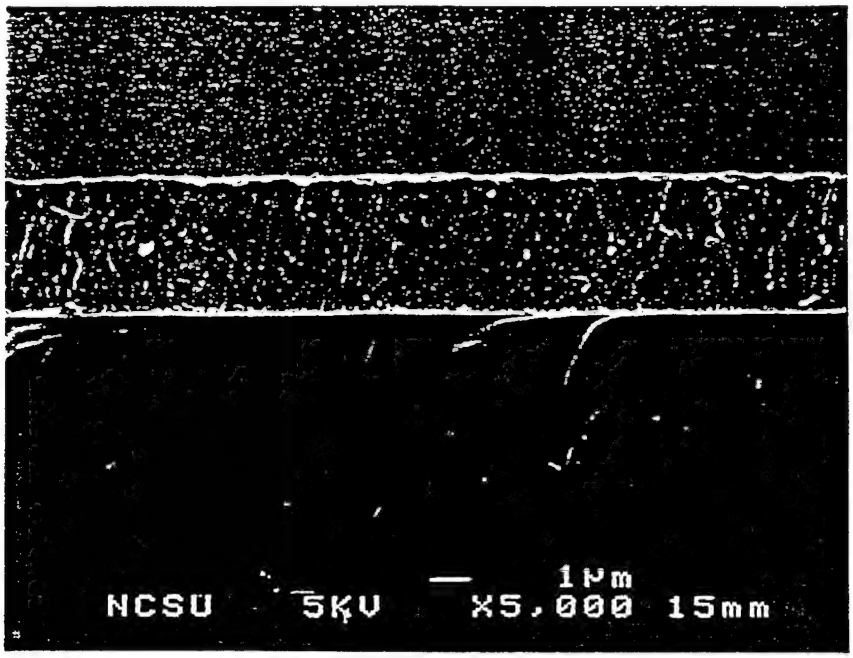

Figure 3. GaN film deposited on Si(111) substrate.

Auger electron spectroscopy revealed that C and O are the major contaminants in the deposited GaN films. Figure 5 compares three spectra take from a GaN film before sputtering, after Ar ion sputtering for 60 seconds and finally after sputtering for 120 seconds total. A reduction in the C and O content after the initial 60 second sputter is indicated in the figure. This is consistent with the removal of a surface contamination layer. The supersonic beam deposition chamber is not connected to the Auger analysis chamber, precluding *in vacuo* transfers and necessitating an in-air transfer that exposes the samples to contaminants.

The spectrum collected after 120 seconds of Ar ion sputtering shows significant C contamination. This last spectrum also shows the presence of Si, indicating that most of the GaN film had been milled away revealing the Si substrate. The fine structure of the C peak is consistent with graphitic C and not SiC. The presence of the C at the film/substrate interface is attributed to C contamination in the deposition system. The chamber is pumped by oil diffusion pumps and oil contamination is always a concern.

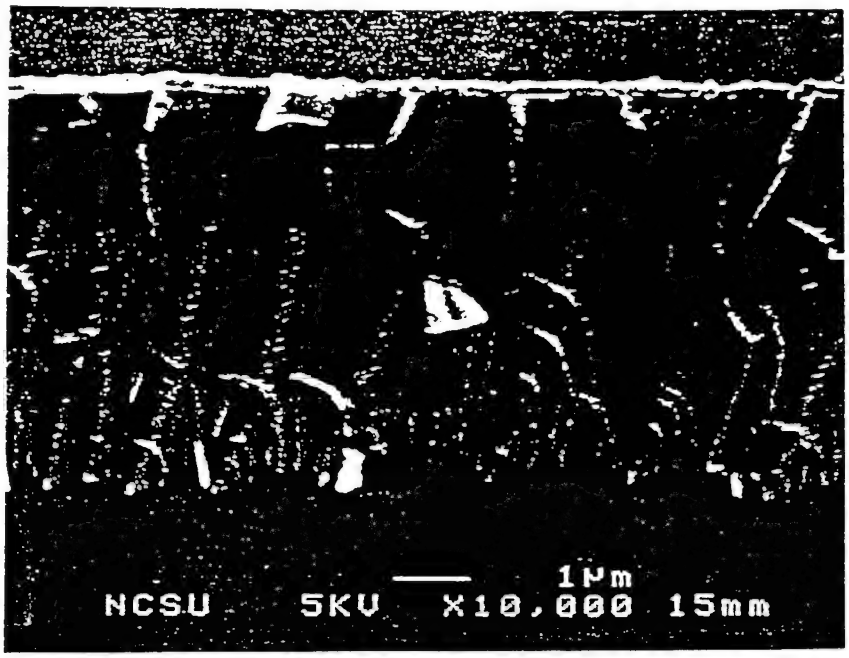

Figure 4. GaN film deposited on $Al_2O_3(0001)$ substrate.

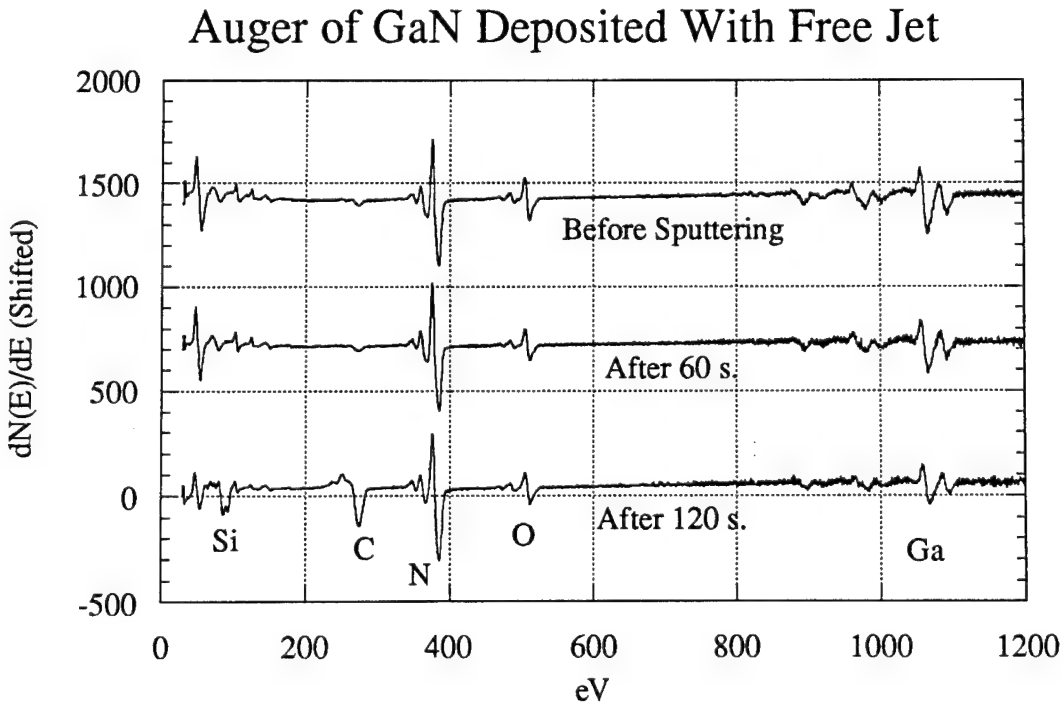

Figure 5. Auger electron spectra collected from GaN film before and after Ar ion sputtering.

System Design. A dual seeded supersonic beam deposition system is currently under construction. This system will contain five chambers: load lock, sample transfer line, beam source chamber, deposition chamber and analysis chamber. A schematic overview of the system is presented in Fig. 6.

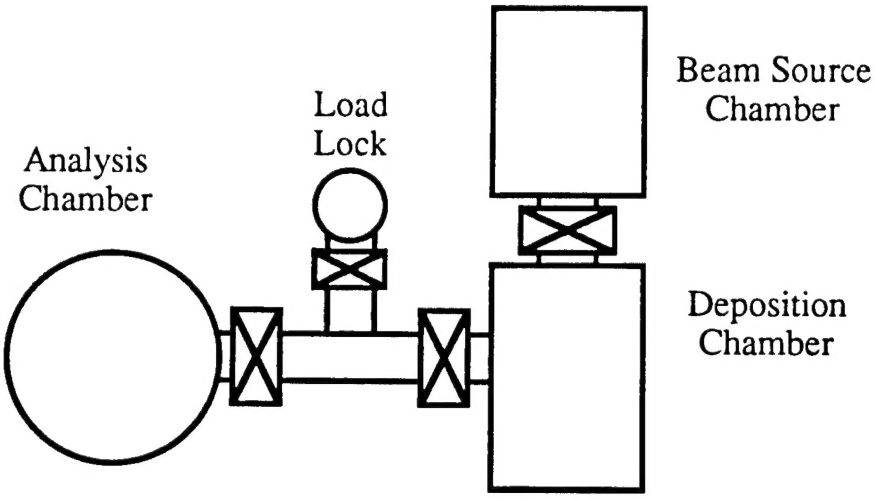

Figure 6. Schematic of dual beam deposition system and analysis chamber.

Samples may be moved through the system as follows:

After the installation of samples, the load lock will be evacuated by a Drytel 31 combination molecular drag-diaphram pump to $<10^{-5}$ Torr before samples can access the sample transfer line.

The sample transfer line is evacuated by a Cryo-pump and permits the movement of samples between the deposition chamber and the analysis chamber under $<10^{-8}$ Torr vacuum.

The deposition chamber is connected to the transfer line and the beam source chamber. A heater stage in this chamber can achieve sample temperatures of ≈600°C. This chamber also contains a RHEED system and a mass spectrometer mounted on a rotatable stage. The mass spectrometer may be configured to perform time of flight measurements of the seeded beams as well as being used for residual gas analysis. Pumping of the deposition chamber will be accomplished with a magnetically levitated combination turbomolecular-molecular drag pump backed by a Fomblinized mechanical pump and an available cryo-cooled titanium sublimation pump. Up to four Knudsen evaporation cells may be fitted to this chamber in addition to an Oxford style R.F. plasma source. Once completely equipped, this versatile chamber may be employed for many varieties of sample cleaning and film deposition processes.

The beam source chamber is divided into two stages: a source stage and a differential pumping stage. Heated nozzles in the first stage generate the supersonic beams which pass through skimmers into the differential pumping stage where the beams are collimated. The

differential pumping stage contains beam flags to interrupt the beams and chopper wheels that may be employed to generate a pulsed beam for time of flight measurements. The collimated beams then are directed into the deposition chamber where they are coincident on the substrate.

The last chamber in the new system is an ultra-high vacuum deposition chamber. The primary analysis technique to be performed in this chamber will be X-ray photoelectron spectroscopy with an angle resolved capability. The configuration of this chamber will also permit the performance of reflectance infrared spectroscopy. This chamber is evacuated by an Ion pump.

D. Conclusions

1. General conditions favoring the deposition of GaN films from a free jet source on Si(111) and Al_2O_3(0001) substrates have been determined.
2. C and O are the major contaminants found in the GaN films.
3. The C and O contaminant appear to be present in the highest concentrations on the film surface and at the film/substrate interface. Inadequate system cleanliness and in-air transfers have been identified as major contaminating agents.
4. A dual beam deposition system has been largely designed and is currently under construction. This versatile system will have the capability of depositing films from dual seeded beams or from a selection of sources including Knudsen cells, gas sources and plasma-assisted gas sources. The system will also offer the capability of performing time of flight measurements, desorption studies, RHEED characterization, XPS, angle resolved XPS and reflectance spectroscopy.

E. Future Plans

1. Install skimmer into single beam system and develop conditions for depositing GaN films using a skimmed, NH_3 seeded He beam.
2. Install TEG jet source in single beam system in an attempt to deposit GaN films with a combination skimmed, NH_3 seeded He beam and free TEG seeded He beam.
3. Continue the design and construction of dual seeded beam deposition system.

F. References

1. J. H. Edgar, J. Mater. Res. **7**, 235 (1992).
2. H. P. Maruska and J. J. Tietjen, Appl. Phys. Lett. **15**, 327 (1969).
   701 (1989).
3. M. J. Paisley, Z. Sitar, J. B. Posthill and R. F. Davis, J. Vac. Sci. and Technol. B **7**, 701 (1989).
4. S. Strite, J. Ruan, Z. Li, A. Salvador, H. Chen, D. J. Smith, W. J. Choyke and H. Martoc, J. Vac. Sci. and Technol. B **9**, 1924 (1991).
5. T. Lei, M. Fanciulli, R. J. Molnar and T. D. Moustakas, Appl. Phys. Lett. **59**, 944 (1991).

6. M. Mizuta, S. Fujieda, Y. Matsumoto and T. Kawamura, Jpn. J. Appl. Phys. **25**, L945 (1986).
7. W. M. Yim, E. J. Stofko, P. J. Zanzucchi, J. I. Pankove, M. Ettenberg and S. L. Gilbert, J. Appl. Phys. **44**, 292 (1973).
8. J. A. Sajurjo, E. Lopez-Cruz, P. Vogh and M. Cardona, Phys. Rev. B **28**, 4579 (1983).
9. H. P. Naruska, D. A. Stevens and J. I. Pankove, Appl. Phys. Lett. **22**, 303 (1973).
10. J. R. Engstrom, D. A. Hansen, M. J. Furjanic and L. Q. Xia, J. Chem. Phys. **99**, 4051 (1993).

VII. Distribution List

Mr. Max Yoder Office of Naval Research Electronics Division, Code: 312 Ballston Tower One 800 N. Quincy Street Arlington, VA 22217-5660	3
Administrative Contracting Officer Office of Naval Research Regional Office Atlanta 101 Marietta Tower, Suite 2805 101 Marietta Street Atlanta, GA 30323-0008	1
Director, Naval Research Laboratory ATTN: Code 2627 Washington, DC 20375	1
Defense Technical Information Center Bldg. 5, Cameron Station Alexandria, VA 22304-6145	2